MORPHOLOGY, FLUCTUATION, METASTABILITY, AND KINETICS IN ORDERED BLOCK COPOLYMERS

Zhen-Gang Wang

Division of Chemistry and Chemical Engineering, California Institute of Technology, Pasadena, California 91125

I. Introduction

Block copolymers are macromolecules consisting of two or more distinct types of linear polymer chains that are connected by covalent bonds. Normally, the distinct chemical blocks tend not to be miscible, yet the chemical bonds that connect them make macroscopic phase separation impossible. These competing effects lead to the fascinating phenomenon of microphase separation in these systems: the spontaneous formation of ordered microstructures with characteristic periodicities in the range of 10–100 nm (Bates and Fredrickson, 1990, 1999). The morphology of the ordered states depends on the composition, the interaction energies between the distinct blocks, and the particular molecular architecture. For simple AB diblock copolymers, as the composition symmetry decreases, a progression from layered lamellae (LAM), through bicontinous gyroid (G), to hexagonally packed cylinders (HEX), and, finally, to body-center-cubic spheres (BCC) is usually followed. The morphological complexity increases drastically when another chemically different block is added. While block copolymers have been traditionally used as bulk thermoplastic materials, the principle of

ADVANCES IN CHEMICAL ENGINEERING, VOL. 28 0065-2377/01 $35.00

microphase ordering in block copolymers is being exploited in novel materials applications, such as nanospheres, fibers, and channels (Ding and Liu, 1998; Liu *et al.,* 1999a,b) and nano-organic/inorganic composites (Förster and Antonietti, 1998; Templin *et al.,* 1998; Avgeropoulos *et al.,* 1998; Chan *et al.,* 1999), as well as optoelectric materials (Morkved *et al.,* 1994; Fink *et al.,* 1997).

From a theoretical standpoint, block copolymers are ideal systems for studying many fundamental issues in the thermodynamics and dynamics of self-assembly of soft materials. This is so because of the relatively large length scale of macromolecules, the slow dynamics associated with the relevant structural relaxations, and the ease of control of the molecular characteristics, such as the molecular weight, compositions, and architecture.

The essential physics leading to microphase ordering in simple diblock copolymers is fairly well understood. For most systems, at elevated temperatures, the free energy is dominated by the configurational entropy, which favors a homogeneous, disordered state. As the temperature decreases, the free energy cost due to unfavorable interaction between the two distinct blocks outweighs the entropic gain in the mixed state, leading to separation of the two blocks, constrained to the size scale of the macromolecule by the connectivity of the polymer chain. Theoretical methods have been developed for a quantitative description of the competing interactions leading to the ordering of block copolymers, as well as of transitions between different morphological structures (Helfand, 1975; Helfand and Wasserman, 1976, 1978, 1980; Leibler, 1980; Semenov, 1985). At the mean-field level, the most significant advance in recent years is the self-consistent field theory of Matsen and Schick (1994). The phase diagram predicted by Matsen and Schick is in good agreement with experimental phase diagrams on model diblock copolymers. In particular, their calculation established, for the first time, the thermodynamic stability of the bicontinuous gyroid phase.

Because of the softness of interactions in block copolymers (here we restrict our consideration to flexible molten blocks above the glass transition temperature), thermal fluctuation in these systems is expected to be significant, especially near the order–disorder transition temperatures (Fredrickson and Helfand, 1987). In addition, the long relaxation times, due to the slowness of the motion of polymers, often lead to metastable and other kinetic states. Thus, full understanding of the self-assembly in block copolymers requires understanding of the nature of fluctuation, metastability, and kinetic pathways for various transitions. Most of this article is focused on theoretical studies of these issues in the simpler AB block copolymers. A key concept that emerges from these studies is the concept of anisotropic fluctuations: first, these fluctuations determine the stability limit of an ordered phase; second, they are responsible for the emergence of new structures

when the initial structure becomes unstable; and third, they are important for consistent interpretation of small-angle neutron or X-ray scattering data in weakly ordered systems.

While the morphology of AB-type block copolymers is limited to a relatively small number of possibilities, the morphology of ABC triblock copolymers is considerably richer and complex (Bates and Fredrickson, 1999). New, exotic, and often unexpected phases are continually being discovered by experimentalists (Breiner *et al.,* 1998). There is a need for theoretical methodology that is capable of predicting, *a priori,* the possible new morphologies in these more complex block copolymers. We describe one such method in this article.

The organization of the rest of the article is as follows: In Section II, we present the general equilibrium theory of anisotropic order parameter fluctuation in the ordered phases of AB-type block copolymers, focusing on the largest fluctuation modes and the scattering patterns due to the fluctuations. The concept of anisotropic fluctuation is then used in Section III to understand the kinetics of various order–order and order–disorder transitions. In Section IV, we show how the theory of anisotropic fluctuation can be used to understand the nature and stability of some nonclassical phases in diblock copolymers. Section V extends our discussion of fluctuation to long wavelengths, where we describe the continuum elasticity description of ordered block copolymer phases and certain long wavelength instabilities. In Section VI, we discuss some of the novel features in ABC triblock copolymers and an efficient method for discovering new ordered phases in these multiblock systems. Section VII contain some brief concluding remarks. The scope of this review is limited to the bulk behavior of flexible block copolymers under quiescent conditions. Many important topics, most notably thin films, surface effects, and flow-induced structures, are left out. These obviously deserve their own articles by experts in the respective fields.

II. Anisotropic Fluctuations in Ordered Phases

Because of the broken translational and rotational symmery, order-parameter fluctuations in ordered phases are anisotropic. The importance of such anisotropic fluctuations was mentioned in the work of Bates and co-workers, who conjectured that anisotropic fluctuations might play a role in stablizing nonclassical ordered structures (Hamley *et al.,* 1993; Bates *et al.,* 1994a,b). The concept was also invoked by this group in understanding the effect of shear on the HEX-to-DIS transitions in diblock copolymer melts (Almdal *et al.,* 1996).

Fluctuation in the order parameter is determined by the free energy change due to variation of the order parameter from its thermal average. For incompressible diblock block copolymer melts, the order parameter is defined as the local volume fraction of A-monomers relative to its global value, $\psi(\vec{r}) = \phi_A(\vec{r}) - f_A$. Because of the periodic nature of the ordered phases, it is more convenient to use the Fourier transform of $\psi(\vec{r})$, which we denote $\psi(\vec{k})$. We separate $\psi(\vec{k})$ into its average value $\psi_0(\vec{k})$ plus a fluctuation part $\Delta\psi(\vec{k})$. To quadratic order in $\Delta\psi(\vec{k})$, the free energy change takes the form of

$$F[\psi(\vec{k})] = F[\psi_0(\vec{k})] + \frac{1}{2}\sum_{\vec{k}}\sum_{\vec{k}'}\Delta\psi(\vec{k})\Gamma(\vec{k},\ \vec{k}')\Delta\psi(\vec{k}'). \tag{1}$$

For periodic structure, the average order parameter can be written $\psi_0(\vec{k}) = \sum_{\vec{G}} A_{\vec{G}}\delta(\vec{k} - \vec{G})$, where $\vec{G}$ is the set of reciprocal lattice wavevectors of the ordered phase, and $A_{\vec{G}}$ is obtained by minimizing the free energy. Taking advantage of the periodicity of the ordered phase, we can write the free energy as

$$F[\psi(\vec{k})] = F[A_{\vec{G}}] + \frac{1}{2}\sum_{\vec{k}}\sum_{\vec{G}}\sum_{\vec{G}'}\Delta\psi(-\vec{k} - \vec{G})\Gamma_{\vec{k}}(\vec{G},\ \vec{G}')\Delta\psi(\vec{k} + \vec{G}'), \tag{2}$$

where $\vec{k}$ is now confined to the first Brillouin zone of the reciprocal space. The nature of fluctuation and the stability of the ordered phase are determined by the matrix $\Gamma_{\vec{k}}(\vec{G},\ \vec{G}')$, which is in general nondiagonal and anisotropic. A stable structure, either locally or globally, is characterized by the positive definiteness of $\Gamma_{\vec{k}}(\vec{G},\ \vec{G}')$. The matrix can be diagonalized to yield a set of eigenvectors and eigenvalues. The ordered phase reaches its spinondal when the lowest eigenvalue turns negative, the corresponding eigenvector dictating the potential direction for the spontaneous emergence of a new structure. When the system is stable, the structure factor can be obtained by inverting the matrix $\Gamma_{\vec{k}}(\vec{G},\ \vec{G}')$.

A rigorous method for calculating the matrix $\Gamma_{\vec{k}}(\vec{G},\ \vec{G}')$ and for addressing anisotropic fluctuations in ordered block copolymer phases at equilibrium was developed by Shi *et al.* (1996), Yeung *et al.* (1996), and Laradji *et al.* (1997a,b) in a series of papers. The theory is based on an expansion of the free energy of an ordered broken symmetry phase around the exact self-consistent field solution of this ordered state. Since the chain conformation in an ordered periodic structure is analogous to the problem of an electron in a periodic potential, the study of order-parameter fluctuations bears an important and useful analogy with the theory of the electronic band structure in crystalline solids. Many of the theoretical concepts and techniques can then be applied to obtain the spectrum of the anisotropic fluctuations.

A simpler though approximate theory for anisotropic fluctuations was developed by Qi and Wang (1997, 1998) based on a Ginzburg–Landau–Leibler free energy approach, valid in the weak segregation regime. In this approach, the anisotropic fluctuation is seen to arise from the coupling between the fluctuation part of the order parameter and the mean-field order parameter. For asymmetric diblock copolymers, the most nontrivial anisotropic fluctuation (near the high-temperature spinodal) is due to the cubic term in the free energy, which contains interaction between the fluctuation and the linear order term of the mean-field order parameter. In the weak segregation limit, both the mean-field order parameter and the fluctuations are dominated by a single wavenumber, k_0. This result, together with the momentum conservation

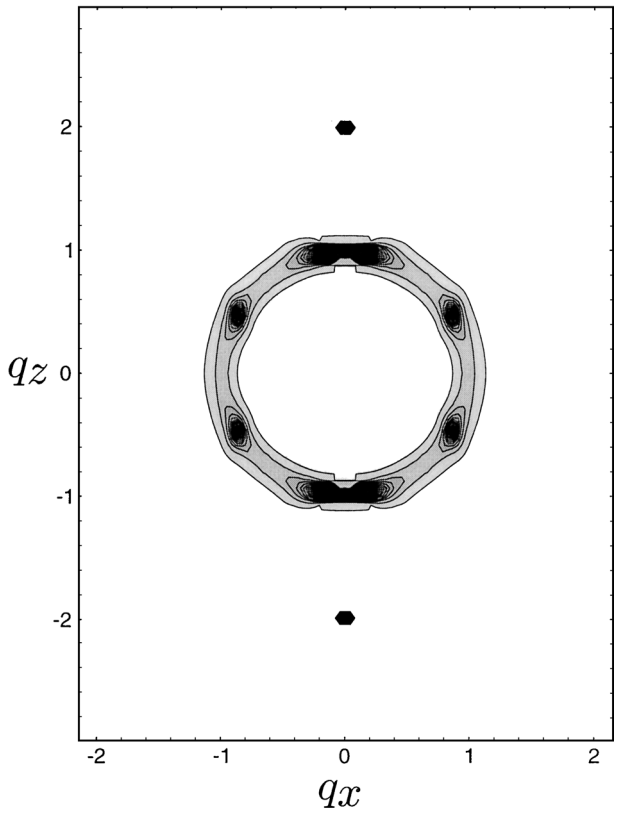

FIG. 1. Scattering pattern of the lamellar phase for a moderately asymmetric diblock copolymer near its spinodal in the $q_y = 0$ scattering plane. The plot shows q_x and q_z in units of k_0. The lamellae are oriented in the z-direction. Courtesy of An-Chang Shi.

that is obeyed in the cubic coupling term, allows one to locate easily the largest fluctuation modes in the reciprocal space.

The scattering function of the lamellar phase near its high-temperature mean-field spinodal is shown in Fig. 1 for the $q_y = 0$ plane. The normal of the lamellar layers is taken to be in the z-direction. In addition to the two strong Bragg peaks at $q_z = k_0$, $q_x = q_y = 0$, and the two higher-order peaks at $q_z = 2k_0$, the most notable new feature is the four peaks at $q_z = k_0/2$, $q_x = (\sqrt{3}/2)k_0$. Because of the rotational symmetry about the z-axis, these four peaks actually correspond to a ring of strong fluctuations at $q_z = k_0/2$. Although this scattering ring lacks any in-layer structure (in the *x, y* plane), the finding that the dominant fluctuations occur at $q_z = k_0/2$ immediately leads to the conclusion that any structures that form as a result of instability of the LAM phase will have a periodicity of two layers in the z-direction. This conclusion has important implications for the kinetics of the LAM-to-HEX transition as well as for understanding the structural nature of the perforated layer phases, as discussed later.

The fluctuations in the HEX phase exhibit similar nontrivial features. Figure 2a shows the real-space contour plot of the order parameter in the

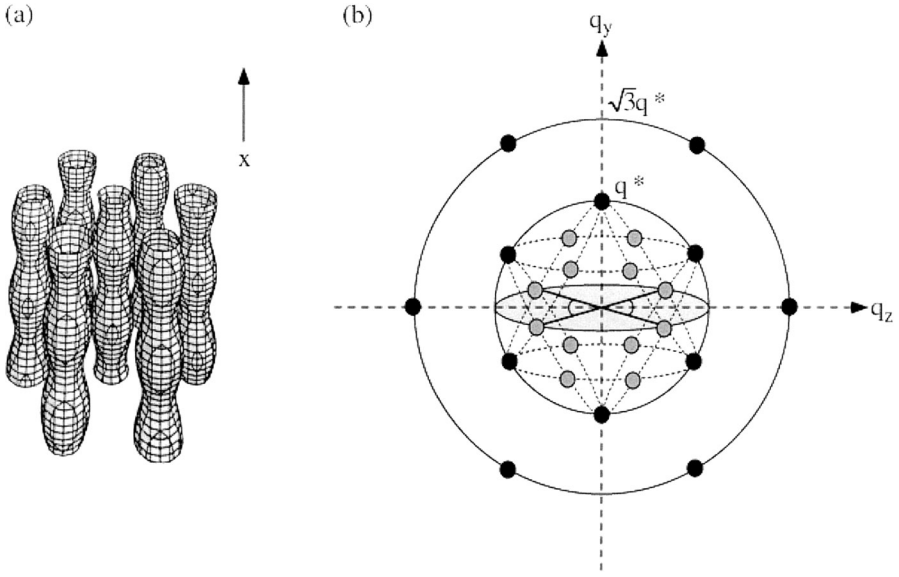

FIG. 2. Dominant fluctuation modes in the HEX phase. (a) Real-space representation according to the work of Laradji *et al.* (1997). (b) Location of the fluctuation peaks, shown as gray dots, in reciprocal space proposed by Qi and Wang (1998). The black dots are the Bragg peaks of the HEX phase. Reproduced with permission from C. Y. Ryu, M. S. Lee, D. A. Hajduk, and T. P. Lodge. *J. Polym. Sci. B Polym. Phys.,* 1998;81:5345–5357.)

HEX phase with the least stable fluctuation modes, following the work of Laradji *et al.* (1997b). Figure 2b demonstrates the location of the largest fluctuation modes in the reciprocal space proposed by Qi and Wang (1998). As the HEX phase approaches its high-temperature spinodal, the largest fluctuation mode leads to undulation of the cylinders. When the amplitudes of the fluctuation become sufficiently high, the undulated cylinders break into ellipsoids centered on the bcc lattice whose [111] direction is along the original cylinders. Qi and Wang (1998) point out that the fluctuation spectrum at the high-temperature spinodal of the HEX phase has the symmetry of a twinned bcc structure rather than the simple bcc structure, as can be seen clearly from Fig. 2b. Experiments by Ryu *et al.* (1997, 1998) on the HEX $\rightarrow$ BCC transition using both small-angle X-ray scattering (SAXS) and transimission electron microscopy (TEM) clearly show the undulation of cylinders as the transition point is approached. These authors term this undulation pretransitional fluctuation. The scattering pattern obtained from the SAXS as well as from Fourier transform of the TEM image is consistent with the twinned bcc structure.

III. Kinetic Pathways of Order–Order and Order–Disorder Transitions

Since the phase boundaries near the order–disorder transition temperature are strongly dependent on temperature, an interesting question naturally arises as to how a system transforms from one morphology to another after a temperature change. In recent years, several groups have experimentally studied the kinetics during the various order–order (Sakurai *et al.,* 1993a,b; Hajduk *et al.,* 1994a; Schulz *et al.,* 1994; Koppi *et al.,* 1994; Kim *et al.,* 1998; Krishnamoorti *et al.,* 2000a,b; Kimishima *et al.,* 2000) and order–disorder (Hashimoto *et al.,* 1986a,b; Singh *et al.,* 1993; Floudas *et al.,* 1996; Adams *et al.,* 1996; Newstein *et al.,* 1998; Balsara *et al,* 1998; Kim *et al.,* 1998) transitions in block copolymers. Qi and Wang (1996, 1997, 1998) performed extensive computer simulation studies of the kinetic pathways of order–order and order–disorder transitions in the direction of temperature jumps. These authors showed, that depending on the extent of the temperature jump, these transitions often occur in several stages and can involve nontrivial intermediate states. For example, it was found that transition from the LAM phase to the HEX phase goes through a perforated lamellar (PL) state within a certain temperature range; see Fig. 3. Extensive experimental studies by Hajduk *et al.* (1997) showed convincingly that the PL, which was previously believed to be a new thermodynamic phase, is a kinetic state *en route* from the LAM to HEX or LAM to G phase, thus providing indirect evidence of the mechanism suggested by the simulation.

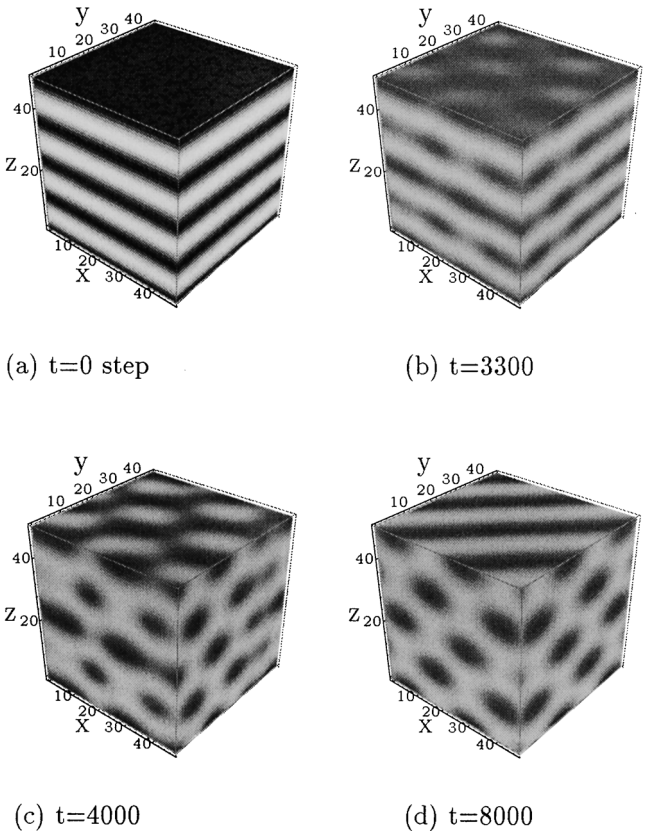

FIG. 3. Computer simulation results using a time-dependent Ginzburg–Landau approach, showing the microstructural evolution after a temperature jump from the lamellar phase to the hexagonal cylinder phase for a moderately asymmetric diblock copolymer. The time units are arbitrary. (Reprinted with permission from *Polymer* 39, S. Y. Qi and Z.-G. Zheng, Weakly segregated block copolymers: Anisotropic fluctuations and kinetics of order-order and order-disorder transitions, 4639–4648, copyright 1998, with permission of Excerpta Medica Inc.)

Qi and Wang also observed a transient undulated HEX state during the melting of the HEX phase to the disordered state. This is consistent with the experimental observation in the shear cessation experiments of Bates and co-workers (Bates *et al.,* 1994a; Almdal *et al.,* 1996). In these experiments, an initially disordered phase of the asymmetric poly(ethylenepropylene-b-ethylethylene) (PEP-PEE) diblock copolymer close to the order–disorder boundary is subjected to a steady shear which induces a transition to the HEX phase. The shear is then suddenly stopped and a transient modulated state is observed as the system relaxes back to the DIS. Insofar as a HEX

phase is created and then the condition is changed to favoring the disordred phase (DIS), the shear-cessation experiment can be likened to a temperature jump.

The appearance of nontrivial intermediate state during the order–order and order–disorder transitions can be understood using the concept of anisotropic fluctuations: the most unstable fluctuation modes lead to the emergence of new structures from the initial phase when that phase becomes unstable. For example, the intermediate states in the LAM-to-HEX transition shown in Fig. 3 is a result of the anisotropic fluctuations located on the spherical shell $q = k_0$ with $q_z = k_0/2$.

Laradji *et al.* (1997a,b) used the most unstable modes of an ordered structure to infer the kinetic pathways in several order–order transitions. Among other things, these authors predict that the LAM-to-HEX and the HEX-to-LAM transitions are not reversible in their kinetic pathways, whereas the transition from LAM to HEX goes through a perforated layer structure, the reverse transition proceeds directly without an intermediate state. Similarly, whereas the HEX-to-BCC transition proceeds directly, the BCC-to-HEX transition is predicted to go through an intermediate modulated layer state. The absence of an intermediate state during the HEX-to-LAM transition was reported in the experiments of Sakurai *et al.* (1993a). The absence of an intermediate state during the HEX-to-BCC transition is in agreement with the simulation result of Qi and Wang (1996, 1997).

The anisotropic fluctuations discussed in the last section refer to fluctuations at equilibrium. However, usually the various order–order and order–disorder transitions are caused by large deviations from equilibrium conditions, which result in large deterministic driving forces given by nonvanishing first derivatives of the free energy. Qi and Wang (1998) performed a linear stability analysis by separating the time-dependent order parameter into a mean-field part and a fluctuation part. The evolution of the meanfield order parameters changes their magnitudes without leading to new structures. Emergence of new structures is associated with fluctuations that lead to deviation from the mean-field path. Qi and Wang calculated the growth rate of the fluctuations as a function of the instantaneous value of the meanfield order parameter and were able to predict at which point along the meanfield path new structures begin to appear. Their analysis also explains why hexagonal cylinders melt uniformly for large temperature jumps but proceed through a BCC modulated hexagonal cylinder state when the temperature jump is small, as observed in their simulation studies. By projecting the order parameter space to a reduced set containing the order parameter of the initial structure and the largest fluctuation modes, they were able to describe qualitatively the full nonlinear evolution of the microstructures in the various transitions.

The concept of anisotropic fluctuations leads to a simple explanation of the epitaxial relationships observed in the transition from one ordered phase to another (Schulz *et al.,* 1994; Koppi *et al.,* 1994). Because of the broken symmetry in a periodically ordered structure, the dominant fluctuation modes reside at specific locations in the reciprocal space, determined by the symmetry of the reciprocal lattice of the initial ordered structure. This spatial relationship is maintained when the new structure—dictated by the most unstable fluctuation modes—grows out of the initial structure, giving rise to the observed epitaxy.

The epitaxial relationship between ordered phases connected by an order–order transition leads to an intriguing phenomenon—the proliferation of HEX cylinder orientations during repeated heating–cooling cycles across the HEX/BCC phase boundary starting from a well-aligned HEX sample. The epitaxy in the HEX-to-BCC transition dictates that the [111] direction of the BCC coincides with the direction of the cylinder axis of the original HEX phase. However, as discussed in the last section, the symmetry of the fluctuation in the HEX is that of a twinned BCC as opposed to a single BCC (Qi and Wang, 1998) (cf. Fig. 2b); thus transition from HEX to BCC should yield two BCC orientations corresponding to the twins. There are four equivalent [111] directions in each of the BCC twins, but one of the four is shared by both, corresponding to the initial cylinder orientation. Therefore, the twins contribute seven distinct [111]-equivalent directions; see Fig. 4. During the reverse transition, each of these directions can become the cylinder direction of the HEX phase. Thus in one cycle of HEX $\rightarrow$ BCC $\rightarrow$ HEX, seven cylinder orientations are generated from a well-aligned HEX with a single cylinder orientation. By the same reasoning, it can be shown that another cycle will give rise to 18 new cylinder directions. Clearly this process can be repeated *ad infinitum,* with each cycle

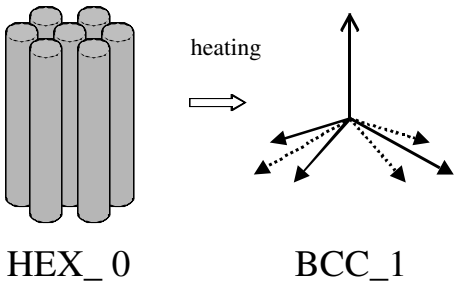

FIG. 4. Seven distinct [111] directions in the BCC phase are produced from a well-aligned HEX phase. These seven [111] directions become the orientations of the cylinders upon cooling back into the HEX phase.

producing more new cylinder directions in a completely deterministic manner. Preliminary SAXS and birefringence data on poly(styrene-b-isoprene) (PS-PI) diblock copolymers support this mechanism (Lee, 2000).

The deterministic proliferation of HEX cylinder orientations during repeated heating–cooling cycles is a unique phenomenon and is a consequence of the fact that the HEX produces a twinned BCC. Indeed, if the HEX-to-BCC transition yielded only a simple BCC structure, then although the first reverse transition would give four cylinder orientations, repeated heating/cooling would not yield any new cylinder orientations since these four directions form a closed set. In contrast, in the LAM $\rightarrow$ HEX transition, the epitaxial relationship only constrains the cylinders to be imbedded in the layers of the minority component of the LAM, but the orientation of the HEX is determined by random fluctuations.

While the foregoing discussions focus primarily on spinodal like kinetics, it is worth mentioning studies that deal with other issues in the order–order and order–disorder transitions. Goveas and Milner (1997) studied the LAM–HEX transition in weakly segregated diblock copolymers by addressing the propagation of the stable phase into the metastable phase. Using an approximate free energy based on the Leibler free energy, these authors obtained the interfacial profile at the propagating front as well as the front velocity. Zhang *et al.* (1997) studied the effects of directional quench from the disordered phase in producing ordered phases that are well oriented. The focus on interfaces and growth in this work complements studies by Shi *et al.* and Qi and Wang which focus on global, spinodal-type kinetics.

Another important issue is that of nucleation/growth kinetics in the order–order and order–disorder transitions. When an ordered morphology is taken beyond its spinodal, transition to another morphology should occur immediately throughout the system. However, some recent experiments on the LAM-to-G transition (Hajduk *et al.,* 1998) and on the HEX-to-BCC transition (Ryu *et al.,* 1997) seem to suggest that the transitions occur by nucleation and growth. Nucleation of the LAM phase from the DIS phase was studied by Fredrickson and Binder (1989). Matsen (1998) recently studied the transition between the HEX and the G phases showing a nucleation/growth mechanism. Whether a transition occurs by spinodal or nucleation/growth depends of course on whether the system is within or beyond the spinodal limit or whether a spinodal exists at all. However, in all order–order transitions, except in the very weak segregation limit, there is mismatch in the lattice spacing of the ordered phases. Such a mismatch would lead to a finite strain in the new ordered phase if the new phase appeared uniformly throughout the system; such a strain could erect a free energy barrier in the transition, thus changing an otherwise spinodal mechanism to a nucleation and growth mechanism. It will be interesting to study how fluctuation

of the order parameter is coupled to lattice distortions. Such phonon-type distortions are discussed in Section IV.

IV. The Nature and Stability of Some Nonclassical Phases

Besides the three classical phases, namely, the LAM, the HEX and the BCC, several complex morphologies have been obtained in experiments. For diblocks with moderate asymmetries, a bicontinuous double-gyroid (G) phase has been commonly observed (Hajduk *et al.,* 1994b, 1995), in which the minority blocks form domains consisting of two interweaving threefold coordinated lattices. The G phase was previously mistaken as the double diamond (D) structure formed from two fourfold coordinated lattices (Thomas *et al.,* 1986). Another complex morphology is the perforated layer (PL) structure (Thomas *et al.,* 1988) observed in the weak-to-intermediate segregation regime of moderately asymmetric diblock copolymers discovered by Bates and co-workers (Hamley *et al.,* 1993; Bates *et al.,* 1994; Förster *et al.,* 1994b; Khandpur *et al.,* 1995).

The thermodynamic stability of the G phase was demonstrated first by Matsen and Schick (1994) using the reciprocal space self-consistent field (SCF) method they developed. It was shown that the G phase is the lowest free energy state compared to the classical phases and the PL and close-packed spheres in certain parts of the phase diagram in the intermediate segregation regime, ending at a triple point with the LAM and the HEX phase on the high-temperature side. Using a larger number of basis functions, Matsen and Bates (1996) studied the phase behavior at stronger segregations; their calculation shows that the G phase become unstable at values of $N\chi > 60$. Matsen and Bates (1997) subsequently performed SCF calculations aimed at a physical understanding of the complex phase behavior of block copolymers in the intermediate segregation regime. They suggested that the competition between chain packing and interfacial tension used to describe the behavior in the strong segregation regime (Semenov, 1985) can also be used to explain the phase behavior in the intermediate segration regime. Interfacial tension prefers the formation of constant mean curvature surfaces to reduce the interfacial area (Thomas *et al.,* 1988), while chain stretching favors domains of uniform thickness. Whereas the classical phases can satisfy both, the complex phases cannot. Of the complex phases considered, only the G phase is least frustrated and is consequently stable at intermediate degrees of segregation.

The calculations mentioned above draw their conclusion about the thermodynamic stability based on comparing free energy among a few candidate

morphologies. They did not address the local stability of the phases. Laradji *et al.* examined the stability of the phases by studying the anisotropic fluctuation. Their calculation shows (Laradji *et al.,* 1997a,b) that the G phase possesses a negative eigenvalue in its fluctuation spectrum, indicating that the G phase may be a saddle point on the free energy surface. This conclusion caused a debate between Matsen (1998) and Laradji *et al.* (1998). No satisfactory resolution of this issue has been reached.

The PL phase discovered by Bates and co-workers was envisioned to consist of alternating minority and majority component layers in which the minority component domains are modulated in thickness or perforated by the majority component with a hexagonal in-plane symmetry. However, the three-dimensional stacking of the layers, i.e., whether they are stacked like abab. . . or abcabc. . . was not established by these researchers. Also, several key features in the small-angle neutron scattering (SANS) data, such as the six weak broad peaks in the in-plane scattering pattern (Hamley *et al.,* 1993; Bates *et al.,* 1994b) as well as the nonsixfold in-plane scattering pattern in some samples (Förster *et al.,* 1994; Khandpur *et al.,* 1995), were never satisfactorily explained. The lack of definitive structural models for the PL led several theoretical calculations (Fredrickson, 1991; de la Cruz *et al.,* 1991; Hamley and Bates, 1994) to assume different structures, which resulted in conflicting conclusions with regard to their thermodynamic stability.

The computer simulation result of Qi and Wang (1997) on the LAM–HEX transition suggested that the PL phase might be a kinetic state between the LAM and the HEX or the G phase. Yeung *et al.* (1996) and Laradji *et al.* (1997a,b) suggested that the PL state is a fluctuating lamellar phase without any specific in-layer structures. A unified description of the structural nature, stability, and possible mechanism of formation of the PL structure in diblock copolymer melts was proposed by Qi and Wang (1997). Using a simple Leibler free energy, it is shown that the PL develops from anisotropic fluctuations in the lamellar phase as it approaches its limit of metastability. Two PL models are proposed, one based on a hexagonal close-packed lattice and the other based on a BCC lattice, with nearly degenerate free energies. In the framework of this free energy, it is found that the PL structure is pseudostable (corresponding to a saddle point in the free energy surface) in the weak segregation limit but can be metastable in the intermediate segregation regime. Their proposed structures produce features that are consistent with all known structural data on the ordered PL phases. In particular, the location and intensity of the in-plane scattering peaks can be understood as arising from anisotropic fluctuations in the metastable PL states, rather than from Bragg scattering.

The stability of the PL morphologies was reexamined by Hajduk *et al.* (1997) in a number of block copolymer melts of low to moderate molecular

weight. Using SAXS and rheological measurements, they showed rather conclusively that the perforated layer structures, which were initially believed to be new equilibrium phases, are long-lived nonequilibrium states which convert to the G or HEX phase upon isothermal annealing. Thus there seems to be agreement between theory and experiments on the stability of the PL state.

V. Long-Wavelength Fluctuations and Instabilities

The ordered phases formed in block copolymer melts are liquid–crystalline mesophases in that they possess properties intermediate between liquids and solids. This is so because of the different degrees of ordering that can take place at two very different length scales: on the microscopic level, the monomeric units possess quite a bit of fluidity, lacking positional order, and yet on length scales larger than the chain size, the system can exhibit long-range periodic structures. This structural regularity implies that the system is capable of sustaining anisotropic elastic deformation. At long length scales, such anisotropic elastic deformation is described in terms of continuum elasticity. For example, the free energy change due to long wavelength deformation in the lamellar phase can be written

$$\Delta F = \frac{1}{2} \int d\vec{r} \left[B \left(\frac{\partial u}{\partial z} \right)^2 + K \left(\nabla_\perp^2 u \right)^2 \right], \tag{3}$$

where $u(\vec{r})$ is the displacement, defined as the change of the layer position at $\vec{r}$ from its equilibrium position, and $\nabla_\perp$ is the gradient operator in the transverse directions to the layer normal. B and K are termed the compressional and bending moduli, respectively. It can be seen that this free energy has the same form as the free energy of deformation in smectic-A liquid crystals (de Gennes and Prost, 1993). Indeed, the long-wavelength deformation of the ordered block copolymer phase can be described in the same way as the deformation in crystalline solids and liquid crystals. More generally, the elastic deformation free energy of a block copolymer mesophase can be written

$$\Delta F = \frac{1}{2} \int d\vec{r} (B_{ijkl} \partial_i u_k \partial_j u_l + K_{ijklmn} \partial_i \partial_j u_m \partial_k \partial_l u_n), \tag{4}$$

where summation of repeated indices is implied. For a given block copolymer mesophase, symmetry arguments can be used to reduced the number of independent deformation modes and hence the number of terms appearing in the above expression (de Gennes and Prost, 1993).

Long-wavelength deformations/fluctuations in block copolymers are important for several reasons. First, they are responsible for the mechanical properties of a block copolymer mesophase. Second, they determine the degree of long-range order and the effects of defects in the ordered phases. Finally, they are responsible for certain novel long-wavelength instabilities.

The key input in the continuum elasticity descprition of long-wavelength deformations is the set of elastic moduli that appear in Eq. (4). Several authors have calculated the elastic moduli for the lamellar phase of block copolymers. Amundson and Helfand (1993) derived the elastic deformation free energy for a lamellar phase in the weak segregation limit starting from a fluctuation renormalized free energy derived by Fredrickson and Binder (1989). Wang (1994) obtained the compressional and binding moduli for the diblock copolymer phases in both the strong and the weak segregation limit and used the results to examine the thermomechanical behavior and stress-induced melting. Chakraborty and Fredrickson (1994) calculated the compressional modulus for a lamellar phase of AB random copolymers in the strong segregation limit, showing a nontrivial dependence on the sequence distribution. Hamley (1994) derived the elastic free energy of the HEX phase in the weak segregation limit and examined the mechanical instabilities under tension. These studies deal with specific ordered block copolymer mesophases in either the weak or the strong segregation regime; extension to more complex morphologies at arbitrary degrees of segregation is not obvious.

A different route for computing the elastic moduli was taken by Yeung *et al.* (1996), who obtained the elastic moduli for symmetric diblock copolymer lamellar by examing the long-wavelength limit of the anisotropic fluctuation spectrum. This procedure is similar to earlier density functional calculation of elastic moduli for crystalline solids (Lipkin *et al.,* 1985). A similar phase Hamiltonian formulation using an approximate density functional was developed by Kawasaki and Ohta (1986) to compute the elastic moduli of the three classical phases of diblock copolymers in the strong segregation limit. However, a common assumption shared by these works is that of affine deformation, which in this context means that the only change in the density profile is through a change in the coordinates induced by the deformation. While such an approximation may not cause significant errors for hard atomistic solids, adjustment of the profile in systems with soft interactions to imposed deformation could have more pronounced effects. Indeed, Matsen (1999) showed that for the bending modulus of a diblock copolymer film separating the A-rich phase from the B-rich phase in an AB binary blend, the assumption of affine deformation can lead to a change in the sign.

Shi and Wang (unpublished work) have recently developed a rigorous theory for extracting the elastic moduli of ordered block copolymer phases

from the anisotropic order-parameter fluctuation spectrum, without invoking the affine deformation assumption. In this new theory, both the phase (displacement) and the amplitudes of the density wave in an ordered block copolymer phase are allowed to vary upon a long-wavelength deformation. A free energy for continuum elasticity is obtained starting from Eq. (2) by integrating the changes in the amplitudes, subject to a given deformation u. In Fourier representation, the resulting elastic free energy takes the form

$$\Delta F = \frac{1}{2} \sum_{\vec{k}} \mathbf{S}^{-1}(\vec{k}) : \vec{u}(\vec{k})\vec{u}(-\vec{k}). \tag{5}$$

The matrix $\mathbf{S}^{-1}$ is a second rank tensor defined as

$$\mathbf{S}^{-1}(\vec{k}) = \sum_{\vec{G}>0} \sum_{\vec{G}'>0} [Q_{\vec{k}}(\vec{G},\ \vec{G}') - R_{\vec{k}}(\vec{G},\ \vec{G}')] A_{\vec{G}} A_{\vec{G}'} \vec{G}\vec{G}', \tag{6}$$

where the functions $Q_{\vec{k}}(\vec{G},\ \vec{G}')$ and $R_{\vec{k}}(\vec{G},\ \vec{G}')$ can be obtained from the matrix $\Gamma_{\vec{k}}(\vec{G},\ \vec{G}')$. $\mathrm{S}^{-1}(\vec{k})$ can be expanded for small k, the quadratic coefficients yielding B_{ijkl} and the quartic coefficient giving K_{ijklmn} in Eq. (4). The $R_{\vec{k}}(\vec{G},\ \vec{G}')$ term reflects the renormalization of the elastic moduli due to the coupling between the amplitude of the density wave and the displacements. Numerical implementation of the method using the exact self-consistent field solutions is quite involved and is now in progress. An interesting and important application of the theory is the study of mechanical properties of the bicontinuous gyroid phase. In addition, the theory can be used to understand the very different degrees of long-range order obtained in the HEX phases on the two sides of the phase diagram in conformational asymmetric diblock copolymers (Gido and Wang, 1997).

The coupling between the displacements and the amplitude of the density wave manifests itself in a long-wavelength instability in ordered phases with soft directions (such as LAM and HEX) upon a temperature quench (Qi and Wang, 1999). This phenomenon is most easily illustrated using the example of the LAM phase in the weak segregation limit. At a temperature T_0 below the order–disorder transition temperature, the density wave can be represented as a simple sinusoidal wave:

$$\psi(\vec{r}) = A_0 \cos\left(\frac{2\pi}{d} z\right), \tag{7}$$

where d is the period of the LAM and we have taken the lamellar normal to be in the z-direction. Upon a decrease in temperature to $T_1 < T_0$ (but still in the weak segregation limit so that the period d remains unchanged), the amplitude will evolve to a new equilibrium value. However, the initial

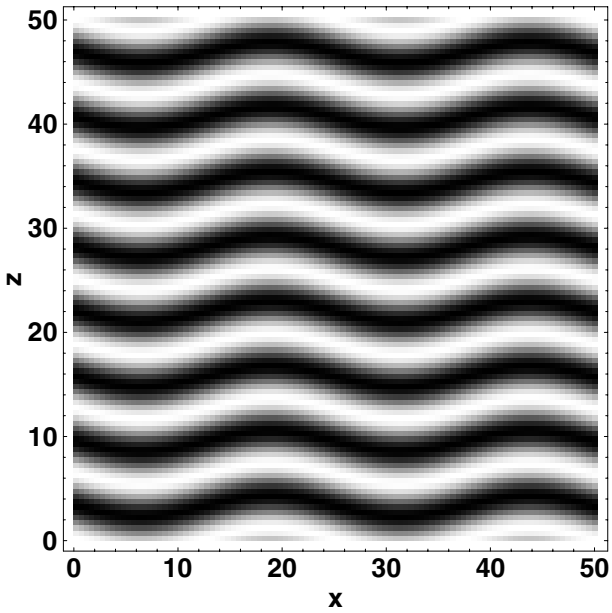

FIG. 5. A two-dimensional illustration of the undulation instability caused by a sudden temperature decrease within the LAM phase.

deviation from equilibrium causes a buckling instability (see Fig. 5), so that the time evolution of the order-parameter takes the form

$$\psi(\vec{r}, t) = A(t) \cos\left[\frac{2\pi}{d}(z - u(\vec{r}, t))\right] \tag{8}$$

while the relaxation of the amplitude A is exponentially fast, the relaxation of u is only algebraic ($\approx t^{-1/4}$). This would lead to a long-lived transient transverse broadening of the Bragg peaks in the scattering function.

A similar instability exists for the HEX phase, resulting in the undulation of the cylinder axes upon a temperature quench (still in the HEX phase). If we take the special case of $A_0 = 0$, our analysis should apply equally to the ordering kinetics after a temperature quench from the disordered state. Thus the predicted instability might be responsible for the unusual kinetics observed by Balsara *et al.* (1998) in a temperature quench from the disordered state to the HEX state for PS-PI copolymer melts. Using a combination of small-angle X-ray scattering and time-resolved depolarized light scattering, they demonstrate that for a large quench depth, hexagonal order occurs before the development of a coherent structure along the cylinder direction

(which they call the liquid direction). They envisage the formation of arrays of hexagonally packed cylinders with a limited persistent length at the initial stage of the transition and subsequent straightening of the cylinders at late stages, with the second process occuring at a much slower rate.

VI. Morphology and Metastability in ABC Triblock Copolymers

In contrast to the simpler AB diblock copolymers, where the morphology is determined by the relative lengths of the two blocks and by a single interaction parameter characterizing the incompatibility of the two blocks (at the mean-field level), the morphology of ABC triblock copolymers depends crucially on the architecture of the triblocks (i.e., A–B–C, C–A–B, or A–C–B, linear vs star) and on the relative strengths of three pair interaction parameters (Gido *et al.,* 1993; Mogi *et al.,* 1993; Sioula *et al.,* 1998a,b). Consequently, the morphology of ABC triblock copolymers is considerably richer and more complex (Auschra and Stadler, 1993; Mogi *et al.,* 1994; Breiner *et al.,* 1998; Brinkman *et al.,* 1998). In the strong segregation limit, several theoretical calculations using the known structures of the ordered block copolymer phases have been carried out (Nakazawa and Ohta, 1993; Stadler *et al.,* 1995; Zheng and Wang, 1995; Phan and Fredrickson, 1998). The calculated phase diagram is in general agreement with experimental results. Werner and Fredrickson (1997) studied the spinodal limit of the disordered state in ABC triblock copolymers and found several cases with reentrant behaviors. Self-consistent field calculations have been performed (Matsen, 1997) to elucidate the nature of the tricontinuous phases in ABC triblock copolymers.

In spite of these successes, and in spite of the high level of sophistication in block copolymer theory, almost all the nontrivial new morphologies were first discovered experimentally. The role of theory has been primarily to compute and compare the free energies for a number of candidate morphologies with presumed symmetries. Therefore, there is a need for theoretical methods capable of discovering or predicting new ordered morphologies. This need becomes particularly acute in view of the large parameter space and the increased number of possible architectures in multiblock copolymers. An important step in this direction was taken recently by Drolet and Fredrickson (1999), who proposed exploring the morphological space by solving the self-consistent field equations in real space and varying the initial conditions. Their method involves discretizing the self-consistent equations on grid points within a fixed volume. To minimize the finite size effects, a large volume (with each dimension several times larger than the typical domain size of the ordered phases) and hence a large number of grid points are required.

Bohbot-Raviv and Wang (2000) developed a similar method with an important improvement over that of Drolet and Fredrickson: instead of minimizing the free energy over a large but fixed volume, the method of Bohbot-Raviv and Wang performs free energy minimization in real space in an arbitrary *unit cell* with respect to the composition profile *and* the dimensions of the unit cell. The use of a unit cell considerably reduces the number of grid points needed for the numerical minimization, while allowing the dimensions of the unit cell to vary, removing any finite size/strain effects that exist in straightforward discretization with a fixed volume. In addition, since the primary focus is on discoverying new structures, rather than accurate evaluation of the free energy, Bohbot-Raviv and Wang constructed a simple, approximate free energy functional where the chain connectivity is retained at the RPA level. This simplification further increases the effciency of their method. Figure 6 shows two complex two-dimensionally ordered new morphologies discovered by this method. Figure 6a is similar to the knitting pattern discovered by Breiner *et al.* (1998). A promising direction is to combine the efficiency of this method with the accuracy of self-consistent field theory, wherein new ordered morphologies identified by the approach of Bohbot-Raviv and Wang serve as input for more elaborate SCF calculations. This combination will provide the long desired

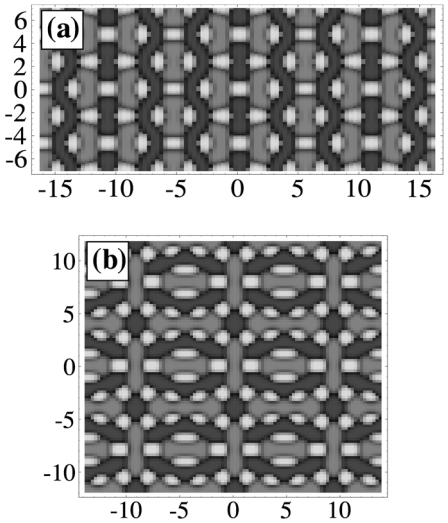

FIG. 6. Complex two-dimensionally ordered ABC triblock copolymer phases produced using the method of Bohbot-Raviv and Wang (2000). The parameters are (a) $f_A = 0.36$, $f_B = 0.31$, $N\chi_{AB} = 30$, $N\chi_{BC} = 32$, and $N\chi_{AC} = 22$; (b) $f_A = 0.36$, $f_B = 0.31$, $N\chi_{AB} = 30$, $N\chi_{BC} = 35$, and $N\chi_{AC} = 22$.

theoretical tool for efficiently and accurately predicting, *a priori,* complex phase diagrams of multiblock copolymer melts.

Because the strengths of the three pair interactions in an ABC triblock are in general unequal and have different temperature dependences, as the temperature is decreased from the disordered (well-mixed) state, segregation will occur first for the most incompatible pair(s). At even lower temperatures, segregation between the other pair(s) of blocks will follow, which is often but not always accompanied by a phase transition, depending on whether a symmetry breaking is involved. This stagewise segregation can give rise to interesting metastable or otherwise kinetically trapped states. An example is given in Fig. 7 for an A–B–C sequenced triblock where the repulsion between the two terminal blocks, A and C, is less than that between the middle block B and the two terminal blocks. Coming from the disordered phase, the first segregation will be between block B and the two terminal blocks, resulting in a two-domain structure (i) with a B domain and a mixed A/C domain. In this domain structure, the chains can assume both loop and bridge conformations, where the bridges can be oriented in either direction. At some lower temperature, the A and C blocks will begin to segregate from each other, eventually resulting in a fully segregated three-domain structure (ii). In such a structure, the triblocks take predominantly

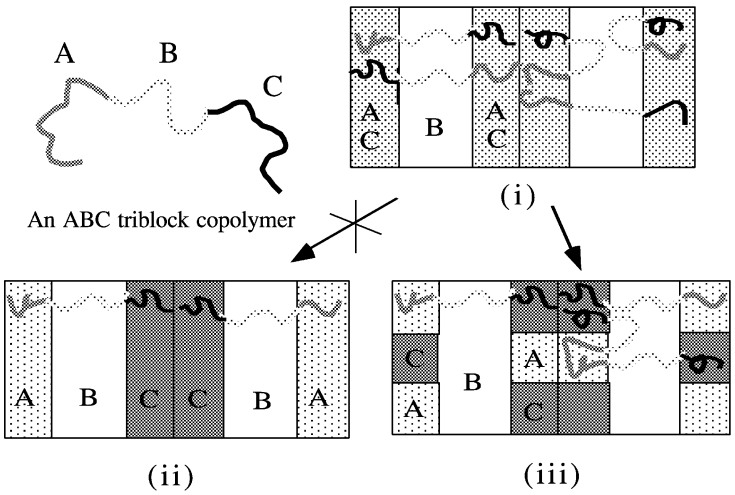

FIG. 7. Transition from a two-domain structure to a three-domain structure in an ABC triblock copolymer lamellar phase. Although state ii is thermodynamically the most stable state, transition to this state from i is hindered because of the high free energy cost in switching the orientation of the bridges and in turning the loops into bridges. Thus, a kinetically more likely process is for the A and C blocks from the bridge conformation to separate laterally, with the loops straddling the interfaces between the A and the C domains.

the bridge conformation. Although state (ii) is thermodynamically the most favorable, the transition from (i) to (ii) is hindered because of the high free energy cost in switching the orientation of the bridges and in turning the loops into bridges. Thus a kinetically more likely process is for the A and C blocks from the bridge conformation to separate laterally, with the loops straddling the interfaces between the A and the C domains (iii). Such a topologically trapped state has been observed by Kornfield's group at Caltech for the S–I–R triblock copolymer (S, polystyrene; I, polyisoprene; R, random styrene–isoprene copolymer).

Figure 8 similarly shows the effects of preordering on the subsequent segregation. The interaction parameters and blocks lengths in both cases are identical to those in Fig. 6b (connected-wheel pattern); the only difference lies in the intial condition. In Fig. 8a, the initial state is that of hexagonally ordered domains of A (gray) in a mixed B/C (dark/light) matrix, while in Fig. 8b a hexagonally ordered C in an A/B matrix is used. Both patterns have retained features of the initial domain structure, though with considerable distortion and modification. Not surprisingly, these kinetically trapped metastable states both have free energies higher than the morphology shown in Fig. 6b. The dependence of these kinetically trapped states on the processing route can be exploited to obtain structures that would otherwise be inaccessible.

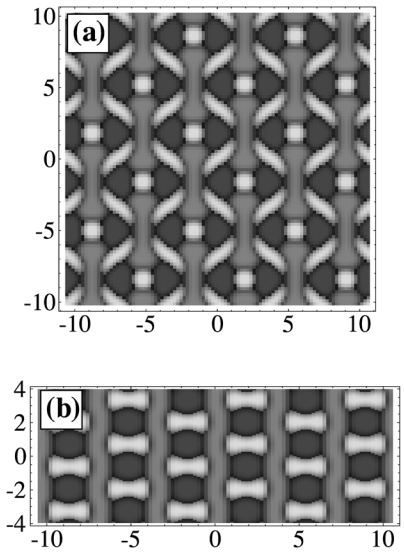

FIG. 8. Metastable states produced from preordered states. The parameters are identical to those used in Fig. 7b.

VII. Conclusions

The microphase ordering in block copolymers is one of the best examples of self-assembly in soft matter and exemplifies many of the principal features of this phenomenon, such as competing interactions and hierachical order (Muthukumar *et al.,* 1997). In contrast to atomic or small molecular systems whose thermodynamic and dynamic properties are governed by strong and detailed interactions at the atomic scale, the effects of such atomic-level interactions on the behaviors of block polymers are usually manifested in an average manner, allowing a coarse-grained description of the systems. As a result, it is often possible to describe accurately the physics of block copolymers in terms of a few course-grained parameters, such as the molecular weight, composition, and Flory–Huggins parameters, which can often be fairly readily controlled experimentally. This, together with the large length scales and slow relaxation times, makes block copolymers ideal model systems for addressing many fundamental issues in the thermodynamic and dynamics in soft self-assembling systems. Our understanding of these issues in block copolymers can often be helpful in understanding related issues in smaller molecular systems, such as in small molecular surfactants (Muller and Schick, 1998; Li and Schick, 2000). On the other hand, topological constraints, and different architectural designs in polymeric systems, lead to unique phenomena such as topologically frustrated states, as well as the formation of complex, exotic ordered phases. These phenomena add new richness to self-assembly and can be utilized in the design of novel materials.

REFERENCES

Adams, J. L., Quiram, D. J., Graessley, W. W., Register, R. A., and Marchand, G. R., *Macromolecules* **29,** 2929–2938 (1996).

Almdal, K., Mortensen, K., Koppi, K. A., Tirrell, M., and Bates, F. S., *J. Phys. II* **6,** 617–637 (1996).

Amundson, K., and Helfand, E., *Macromolecules* **26,** 1324–1332 (1993).

Auschra, C., and Stadler, R., *Macromolecules* **26,** 2171–2174 (1993).

Avgeropoulos, A., Chan, V. Z. H., Lee, V. Y., Ngo, D., Miller, R. D., Hadjichristidis, N., and Thomas, E. L., *Chem. Mater.* **10,** 2109–2115 (1998).

Balsara, N. P., Garetz, B. A., Newstein, M. C., Bauer, B. J., and Prosa, T. J., *Macromolecules* **31,** 7668–7675 (1998).

Bates, F. S., and Fredrickson, G. H., *Annu. Rev. Phys. Chem.* **41,** 525–557 (1990).

Bates, F. S., and Fredrickson, G. H., *Phys. Today* **52,** 32–38 (1999).

Bates, F. S., Koppi, K. A., Tirrell, M., Almdal, K., and Mortensen, K., *Macromolecules* **27,** 5934–5936 (1994a).

Bates, F. S., Schulz, M. F., Khandpur, A. K., Frster, S., and Rosedale, J. H., *Faraday Discuss.* **98,** 7–18 (1994b).
Bohbot-Raviv, Y., and Wang, Z.-G., *Phys. Rev. Lett.* **85,** 3428–3431 (2000).
Breiner, U., Krappe, U., Thomas, E. L., and Stadler, R., *Macromolecules* **31,** 135–141 (1998).
Brinkmann, S., Stadler, R., and Thomas, E. L., *Macromolecules* **31,** 6566–6572 (1998).
Chan, V. Z. H., Hoffman, J., Lee, V. Y., Iatrou, H., Avgeropoulos, A., Hadjichristidis, N., Miller, R. D., and Thomas, E. L., *Science* **286,** 1716–1719 (1999).
Chakraborty, A. K., and Fredrickson, G. H., *Macromolecules* **27,** 7079–7084 (1994).
de Gennes, P.-G., and Prost, J., *The Physics of Liquid Crystals,* Claredon Press, Oxford, 1993.
de la Cruz, M. O., Mayes, A. M., and Swift, B. W., *Macromolecules* **25,** 944–948 (1991).
Ding, J. F., and Liu, G. J., *Chem. Mater.* **10,** 537–542 (1998).
Drolet, F., and Fredrickson, G. H., *Phys. Rev. Lett.* **83,** 4317–4320 (1999).
Fink, Y., Urbas, A. M., Bawendi, M. G., Joannopoulos, J. D., and Thomas, E. L., *J. Lightwave Technol.* **17,** 1963–1969 (1999).
Floudas, G., Pispas, S., Hadjichristidis, N., Pakula, T., and Erukhimovich, I., *Macromolecules* **29,** 4142–4154 (1996).
Förster, S., and Antonietti, M., *Adv. Mater.* **10,** 196–218 (1998).
Förster, S., Khandpur, A. K., Zhao, J., Bates, F. S., Hamley, I. W., Ryan, A. J., and Bras, W., *Macromolecules* **27,** 6922–6935 (1994).
Fredrickson, G. H., *Macromolecules* **24,** 3456–3458 (1991).
Fredrickson, G. H., and Binder, K., *J. Chem. Phys.* **91,** 7265–7275 (1989).
Fredrickson, G. H., and Helfand, E., *J. Chem. Phys.* **87,** 697–705 (1987).
Gido, S. P., and Wang, Z.-G., *Macromolecules* **30,** 6771–6782 (1997).
Gido, S. P., Schwark, D. W., Thomas, E. L., and do Carmo, G. M., *Macromolecules* **26,** 2636–2640 (1993).
Goveas, J. L., and Milner, S. T., *Macromolecules* **30,** 2605–2612 (1997).
Hajduk, D. A., Gruner, S. M., Rangarajan, P., Register, R. A., Fetters, L. J., Honeker, C., Albalak, R. J., and Thomas, E. L., *Macromolecules* **27,** 490–501 (1994a).
Hajduk, D. A., Harper, P. E., Gruner, S. M., Honeker, C. C., Kim, G., Thomas, E. L., and Fetters, L., *Macromolecules* **27,** 4063–4075 (1994b).
Hajduk, D. A., Harper, P. E., Gruner, S. M., Honeker, C. C., Thomas, E. L., and Fetters, L. J., *Macromolecules* **28,** 2570–2573 (1995).
Hajduk, D. A., Takenouchi, H., Hillmyer, M. A., Bates, F. S., Vigild, M. E., and Almdal, K., *Macromolecules* **30,** 3788–3795 (1997).
Hajduk, D. A., Ho, R. M., Hillmyer, M. A., and Bates, F. S., *J. Phys. Chem. B* **102,** 1356–1363 (1998a).
Hajduk, D. A., Tepe, T., Takenouchi, H., Tirrell, M., Bates, F. S., Almdal, K., and Mortensen, K., *J. Chem. Phys.* **108,** 326–333 (1998b).
Hamley, I. W., *Phys. Rev. E* **50,** 2872–2880 (1994).
Hamley, I. W., and Bates, F. S., *J. Chem. Phys.* **100,** 6813–6817 (1994).
Hamley, I. W., Koppi, K., Rosedale, J. H., Bates, F. S., Almdal, K., and Mortensen, K., *Macromolecules* **26,** 5959–5970 (1993).
Hashimoto, T., Kowsaka, K., Shibayama, M., and Suehiro, S., *Macromolecules* **19,** 750–754 (1986a).
Hashimoto, T., Kowsaka, K., Shibayama, M., and Kawai, H., *Macromolecules* **19,** 754–762 (1986b).
Helfand, E., *Macromolecules* **8,** 552–556 (1975).
Helfand, E., and Wasserman, Z. R., *Macromolecules* **9,** 879–888 (1976).
Helfand, E., and Wasserman, Z. R., *Macromolecules* **11,** 960–966 (1978).
Helfand, E., and Wasserman, Z. R., *Macromolecules* **13,** 994–998 (1980).

Kawasaki, K., and Ohta, T., *Physica A* **139,** 223–255 (1986).
Khandpur, A. K., Förster, S., Bates, F. S., Hamley, I. W., Ryan, A., Bras, W., Almdal, K., and Mortensen, K., *Macromolecules* **28,** 8796–8806 (1995).
Kim, J. K., Lee, H. H., Gu, Q. J., Chang, T., and Jeong, Y. H., *Macromolecules* **31,** 4045–4548 (1998).
Kimishima, K., Koga, T., and Hashimoto, T., *Macromolecules* **33,** 968–977 (2000).
Koppi, K. A., Tirrell, M., and Bates, F. S., *Phys. Rev. Lett.* **70,** 1449–1452 (1993).
Koppi, K. A., Tirrell, M., Bates, F. S., Almdal, K., and Mortensen, K., *J. Rheol.* **38,** 999–1027 (1994).
Krishnamoorti, R., Silva, A. S., Modi, M. A., and Hammouda, B., *Macromolecules* **33,** 3803–3809 (2000a).
Krishnamoorti, R., Modi, M. A., Tse, M. F., and Wang, H. C., *Macromolecules* **33,** 3810–3817 (2000b).
Lammertink, R. G. H., Hempenius, M. A., van den Enk, J. E., Chan, V. Z. H., Thomas, E. L., and Vancso, G. J., *Adv. Mater.* **12**(2), 98–103 ((2000).
Laradji, M., Shi, A. C., Desai, R. C., and Noolandi, J., *Phys. Rev. Lett.* **78,** 2577–2580 (1997a).
Laradji, M., Shi, A. C., Noolandi, J., and Desai, R. C., *Macromolecules* **30,** 3242–3255 (1997b).
Laradji, M., Desai, R. C., Shi, A. C., and Noolandi, J., *Phys. Rev. Lett.* **80,** 202–202 (1998).
Lee, H. H., *The Kinetics and Mechanism of Order to Order Transition in Block Copolymers,* Ph.D. thesis, Pohang University of Science and Technology, Pohang, Korea, 2000.
Leibler, L., *Macromolecules* **13,** 1602–1617 (1980).
Li, X. J., and Schick, M., *Biophys. J.* **78,** 34–46 (2000).
Lipkin, M. D., Rice, S. A., and Mohanty, U., *J. Chem. Phys.* **82,** 472–479 (1985).
Liu, G. J., Ding, J. F., Hashimoto, T., Kimishima, K., Winnik, F. M., and Nigam, S., *Chem. Mater.* **11,** 2233–2240 (1999a).
Liu, G. J., Ding, J. F., Qiao, L. J., Guo, A., Dymov, B. P., Gleeson, J. T., Hashimoto, T., and Saijo, K., *Chem.-Eur. J.* **5,** 2740–2749 (1999b).
Matsen, M. W., *Phys. Rev. Lett.* **80,** 201–201 (1998a).
Matsen, M. W., *Phys. Rev. Lett.* **80,** 4470–4473 (1998b).
Matsen, M. W., *J. Chem. Phys.* **108,** 785–796 (1998c).
Matsen, M. W., *J. Chem. Phys.* **110,** 4658–4667 (1999).
Matsen, M. W., and Bates, F. S., *J. Chem. Phys.* **106,** 1–13 (1997).
Matsen, M. W., and Schick, M., *Phys. Rev. Lett.* **72,** 2660–2663 (1994).
Matsen, M. W., and Bates, F. S., *Macromolecules* **29,** 1091–1098 (1996).
Mogi, Y., Mori, K., Kotusji, H., Matsushita, Y., Noda, I., and Han, C. C., *Macromolecules* **26,** 5169–5173 (1993).
Mogi, Y., Nomura, M., Kotusji, H., Ohnishi, K., Matsushita, Y., and Noda, I., *Macromolecules* **27,** 6755–6760 (1994).
Morkved, T. L., Wiltzius, P., Jaeger, H. M., Grier, D. G., and Witten, T. A., *Appl. Phys. Lett.* **64,** 422–424 (1994).
Muller, M., and Schick, M., *Phys. Rev. E* **57,** 6973–6978 (1998).
Muthukumar, M., Ober, C. K., and Thomas, E. L., *Science* **277,** 1225–1232 (1997).
Nakazawa, H., and Ohta, T., *Macromolecules* **26,** 5503–5511 (1993).
Newstein, M. C., Garetz, B. A., Balsara, N. P., Chang, M. Y., and Dai, H. J., *Macromolecules* **31,** 64–76 (1998).
Phan, S., and Fredrickson, G. H., *Macromolecules* **31,** 59–63 (1998).
Qi, S. Y., and Wang, Z.-G., *Phys. Rev. Lett.* **76,** 1679–1682 (1996).
Qi, S. Y., and Wang, Z.-G., *Phys. Rev. E* **55,** 1682–1697 (1997a).
Qi, S. Y., and Wang, Z.-G., *Macromolecules* **30,** 4491–4497 (1997b).
Qi, S. Y., and Wang, Z.-G., *Polymer* **39,** 4639–4648 (1998).

Qi, S. Y., and Wang, Z.-G., *J. Chem. Phys.* **111,** 10681–10688 (1999).
Ryu, C. Y., Lee, M. S., Hajduk, D. A., and Lodge, T. P., *J. Polym. Sci. B Polym. Phys.* **35,** 2811–2823 (1997).
Ryu, C. Y., Vigild, M. E., and Lodge, T. P., *Phys. Rev. Lett.* **81,** 5354–5357 (1998).
Sakurai, S., Kawada, H., and Hashimoto, T., *Macromolecules* **26,** 5796–5802 (1993a).
Sakurai, S., Momii, T., Taie, K., Shibayama, M., Nomura, S., and Hashimoto, T., *Macromolecules* **26,** 485–491 (1993b).
Schulz, M. F., Bates, F. S., Almdal, K., and Mortensen, K., *Phys. Rev. Lett.* **73,** 86–89 (1994).
Semenov, A. N., *Sov. Phys. JETP* **61,** 733–742 (1985).
Shi, A. C., Noolandi, J., and Desai, R. C., *Macromolecules* **29,** 6487–6504 (1996).
Singh, M. A., Harkless, C. R., Nagler, S. E., Shannon, R. F., and Ghosh, S. S., *Phys. Rev. B* **47,** 8425–8435 (1993).
Sioula, S., Hadjichristidis, N., and Thomas, E. L., *Macromolecules* **31,** 5272–5277 (1998a).
Sioula, S., Hadjichristidis, N., and Thomas, E. L., *Macromolecules* **31,** 8429–8432 (1998b).
Stadler, R., Auschra, C., Beckmann, J., Krappe, U., Voigtmartin, I., and Leibler, L., *Macromolecules* **28,** 3080–3097 (1995).
Templin, M., Franck, A., Duchesne, A., Leist, H., Zhang, Y. M., Ulrich, R., Schadler, V., and Wiesner, U., *Science* **278,** 1795–1798 (1997).
Thomas, E. L., Alward, D. B., Kinning, D. J., Martin, D. C., Handlin, D. L., and Fetter, L. J., *Macromolecules* **19,** 2197–2202 (1986).
Thomas, E. L., Anderson, D. M., Henkee, C. S., and Hoffman, D., *Nature* **334,** 598–601 (1988).
Wang, Z.-G., *J. Chem. Phys.* **100,** 2298–2309 (1994).
Werner, A., and Fredrickson, G. H., *J. Polym. Sci. Pol. Phys.* **35,** 849–864 (1997).
Yeung, C., Shi, A. C., Noolandi, J., and Desai, R. C., *Macromol. Theory Simul.* **5,** 291–298 (1996).
Zhang, H. D., Zhang, J. W., Yang, Y. L., and Zhou, X. D., *J. Chem. Phys.* **106,** 784–792 (1997).
Zheng, W., and Wang, Z.-G., *Macromolecules* **28,** 7215–7223 (1995).